Research on Chemical Intermediates
https://doi.org/10.1007/s11164-018-3702-8

A magnetically recoverable copper–salen complex as a nano-catalytic system for amine protection via acetylation using thioacetic acid

Elahe Yazdani[1] · Maryam Kazemi Miraki[1] · Arefe Salamatmanesh[1] · Jamshid Azarnia[1] · Kobra Azizi[1] · Leila Ghandi[1] · Akbar Heydari[1]

Received: 20 August 2018 / Accepted: 5 December 2018

Abstract

A novel copper(II)–salen complex was immobilized on the surface of magnetite nanoparticles using chitosan as a linker. This system exhibits superior catalytic activity in acetyl protection of various amines with thioacetic acid as the acetylating reagent. The method has advantages over others in high selectivity, simple work-up, green reaction medium and the application of an easily recoverable heterogeneous catalyst.

Keywords Thioacetic acid · Copper–salen complex · Magnetite · Nano catalyst · *N*-Acetylation

Introduction

Amines are a beneficial class of compounds which are used as bioactive compounds, dyes and especially synthetic intermediates in the manufacture of many pharmaceutically active ingredients [1–4]. Due to the presence of a lone electron pair, amines can act as both nucleophiles and bases. Alkylation, the Schotten–Baumann reaction, imine/enamine formation and oxidation are mentioned examples in the literature [5–11]. Hence, because of their significant nucleophilicity, it is unavoidable to protect amine functional groups in the presence of other nucleophilic functionalities (e.g., OH, S, P, etc.) to exclude side reactions [12–15]. Generally, the protecting groups are electron-withdrawing substituents,

This article is dedicated to memory of Hasan Rahimi.

Electronic supplementary material The online version of this article (https://doi.org/10.1007/s11164-018-3702-8) contains supplementary material, which is available to authorized users.

✉ Akbar Heydari
heydar_a@modares.ac.ir

[1] Chemistry Department, Tarbiat Modares University, P.O. Box 14155-4838, Tehran, Iran

Published online: 09 January 2019

intended to decrease the nucleophilicity of the nitrogen atom. Thus, classically, the amino group is protected with (1) carboxylic acid-derived groups such as formyl, trifluoroacetyl, phthaloyl, acetoacetyl, maleoyl, chloroacetyl and 2-nitrobenzoyl, and (2) urethane-type protecting groups like benzyloxycarbonyl (Cz, Bz), furfuryloxycarbonyl (Foc), pyridine-4-methoxycarbonyl (Inc) and tert-butyloxycarbonyl (Boc) [16]. Among various methods for the protection of amines, the acetyl moiety is one of the most employed ones [17]. Acetyl chloride and acetic anhydride are widely applied reagents for the acetyl protection of amines. The protocols normally comprise either basic or acidic catalysts [18–28]. In spite of the popularity of these reagents in classical organic synthesis, there are inherited problems associated with the mentioned reagents, such as sensitivity to moisture, the possibility of side reactions and violent reactivity [29].

Thioacetic acid is an organosulfur analogue of acetic acid. It is usually employed for the introduction of a thiol group in molecules. The compound is a yellow liquid which is readily soluble in water [30]. Recently, thioacids have attracted considerable interest in peptide science, as well as in native chemical ligiation [31–40]. Moreover, Gopi et al. [41] reported selective acetyl protection of amines using thioacetic acid in the presence of copper(II) acetate as catalyst. However, recycling of the catalyst in this system is quite cumbersome. Furthermore, there is a possibility for product contamination with metal ions, which might be hazardous in pharmaceutical and natural product syntheses. Although there are more recent reports of using thioacetic acid [42] (or its potassium salt [43]), a more efficient protocol is still required, because this method suffers from the use of various reagents, long reaction times and not being economically viable.

Magnetic nanoparticles are considered as valuable supports for the embedding of various organocatalysts and metals due to their high efficiency and easy separation from the reaction mixture by applying an external magnet, which eliminates tedious and time-consuming filtration or centrifugation [44].

Schiff bases have been intensively explored as ligands and have played important roles in the development of coordination chemistry and catalysis. Schiff bases are typically prepared via the condensation of a primary amine with an aldehyde or ketone [45]. Schiff base–metal complexes have been used as catalysts in many organic transformations such as epoxidation of olefins [46], hydrogenation of organic substrates [47], asymmetric ring opening of terminal epoxides [48] conversion of epoxides into halohydrins [49], oxidation reactions [50], synthesis of pyridopyrazine and quinoxaline derivatives, and cross-coupling reactions [51].

Chitosan, a linear polysaccharide of glucosamine, is the product of deacetylation of chitin in alkaline media. The natural source of chitin is the exoskeleton of shrimps and crabs [52]. Therefore, chitosan is highly biodegradable and environmentally benign [53].

As the progress of our recent researches on environmentally friendly catalytic systems [54–58], we devised a nanocatalyst, taking advantage of the easy separation of magnetic nano-catalysts, the powerful complexing nature of Schiff bases, and the green character of chitosan, to heterogenize copper(II) ion to be applied in the acetyl protection of amines using thioacetic acid.

Experimental section

All chemicals and solvents were purchased from commercial suppliers and used without further purification. FT-IR spectra were obtained over the region 400–4000 cm^{-1} with a Nicolet IR100 FT-IR with spectroscopic grade KBr. XRD patterns were obtained at room temperature with a Philips X-pert 1710 diffractometer with Co Kα ($\lambda = 1.78897$ Å), 40 kV voltage, 40 mA current and in the range 10°–90° (2θ) with a scan speed of 0.020 s^{-1}. Scanning electron microscopy (Philips XL 30 and S-4160) was used to study the catalyst morphology and size. Magnetic saturation of the catalyst was investigated using a vibrating magnetometer/alternating gradient force magnetometer (VSM/AGFM; MDK, Iran). Thermogravimetric analysis was conducted using a thermal analyser with a heating rate of 20 °C min^{-1} over a temperature range of 25–1100 °C underflowing nitrogen. 1H NMR spectra were recorded with a Bruker Advance (DRX 500 MHz, DRX 250 MHz, DRX 400 MHz) in pure deuterated dimethylsulfoxide and chloroform (Sigma) solvent with tetramethylsilane as internal standard.

Preparation of Cu(II)–salen complex

Preparation of chitosan-TCT adduct (Cb1)

Amounts of 1 g of chitosan and 10 mmol of cyanuric chloride (TCT) were stirred in toluene (10 mL) under reflux for 24 h [59]. The resulting product (2 g) was filtered and washed with ethanol and dried at 50–60 °C overnight.

Preparation of chitosan-TCT-En adduct (Cb2)

An amount of 0.5 g of Cb1 was dispersed in 2 mL of ethylene diamine and stirred under reflux for 24 h [59]. The obtained solid (0.7 g) was separated by filtration with subsequent washing with ethanol. It was dried at 60 °C for 12 h to be used in the next step.

Preparation of chitosan-TCT-salen ligand (Cb3)

An amount mof 10 mmol of salicylaldehyde was added to a suspension of 0.5 g of Cb2 in 10 mL methanol and 10 mL glacial acetic acid. The resulting mixture was refluxed for 24 h. The product (Cb3, 1.1 g) was filtered, washed with ethanol and acetone, and then dried at 80 °C for 3 h.

Preparation of chitosan-TCT-salen–Cu(II) complex(Cb4)

An amount of 0.5 g of prepared ligand was dispersed in 20 mL of methanol followed by stepwise addition of 2 mmol $CuCl_2$ and 1 mmol KOH. The mixture

was stirred under reflux for 6 h. Finally, the resultant solid (0.64 g) was filtered, washed with water and acetone, and dried at 80 °C for 3 h.

Preparation of magnetite nanoparticles

Magnetite nanoparticles were prepared according to the previously reported literature [65]. To a vigorously stirred solution of 10 mmol $FeCl_3 \cdot 6H_2O$ and 5 mmol $FeCl_2 \cdot 4H_2O$ in 40 mL deionized water at 80 °C, 10 mL of aqueous ammonia solution (25%W/W) was added in small portions. After 2 h, the resulting black solid was magnetically filtered and washed several times with water till reaching pH 7. Then, the nanoparticles were washed twice with ethanol and dried at ambient temperature.

Preparation of γ-Fe_2O_3 nanoparticles

Magnetite nanoparticles, prepared according to the previous section, were calcined at 300 °C in a vacuum for 3 h to obtain γ-Fe_2O_3@SiO_2.

Preparation of Fe_3O_4@SiO_2 nanoparticles

A coating of a layer of silica on the surface of the Fe_3O_4 nanoparticles was achieved through hydrolysis of tetraethyl orthosilicate (TEOS), 2 mL of which was added to the reaction flask containing the mixture of "Preparation of magnetite nanoparticles" section and EtOH (40 mL), and the mixture was continuously stirred overnight at 40 °C. After decanting by a permanent magnet, the silica-coated nanoparticles were washed three times with hot EtOH and dried at room temperature overnight.

Preparation of γ-Fe_2O_3@SiO_2 nanoparticles

The silica-coated magnetic nanoparticles prepared according to the previous section were calcined at 300 °C in a vacuum for 3 h to obtain γ-Fe_2O_3@SiO_2.

Preparation of Fe_3O_4@TiO_2 nanoparticles

A TiO_2 layer was deposited on the magnetite nanoparticles according to a same procedure as in "Preparation of γ-Fe_2O_3 nanoparticles" section, in which titanium(IV) isopropoxide was used instead of TEOS.

Preparation of γ-Fe_2O_3@TiO_2 nanoparticles

Titania-coated magnetic nanoparticles prepared according to the previous section were calcined at 300 °C in a vacuum for 3 h to obtain γ-Fe_2O_3@TiO_2.

Immobilization of chitosan-TCT-Salen–Cu(II) complex on magnetite nanoparticles

An amount of 1 g of freshly prepared magnetite nanoparticles was dispersed in 20 mL slightly acidified water (10% w/w AcOH). Then, 0.5 g of the Cu(II) complex was added to the mixture and stirred for 12 h at room temperature. The resulting nanoparticles were washed with methanol, water and diethyl ether and dried at room temperature overnight.

General procedure for *N*-acetylation reaction

To a mixture of amine (1.0 mmol, 0.093 for aniline) and thioacetic acid (1.0 mmol, 0.076 g) in water (1 mL), the catalyst (40 mg) was added. The suspension was stirred for 5 min at ambient temperature, and the reaction progress was monitored using thin layer chromatography. After the reaction was considered complete, when the starting material was totally consumed, the catalyst was removed from the reaction mixture with a permanent magnet. The reaction vessel was washed several times with water and methanol. The reaction mixture was extracted from the aqueous mixture with EtOAc (3 × 10 mL) and dried with Na_2SO_4. After evaporation of the solvent under vacuum, the crude product was obtained which could be further purified with recrystallization from ethanol.

Selected spectra of the products

N-phenylacetamide (Table 1, **3a**, see later): White solid; Isolated yield = 85%; mp: 110–112 °C; IR (KBr) ν (cm^{-1}) = 3293, 2924, 2855, 1662, 1603, 1549, 1495, 1433, 1317, 1259, 753. ^{1}H NMR (500 MHz, DMSO-d_6): δ_H (ppm) = 9.92 (s, 1H), 7.57 (d, J = 7.5 Hz, 2H), 7.27 (t, J = 7.5 Hz, 2H), 7.00 (t, J = 7.5 Hz, 1H), 2.03 (s, 3H).

N-(2-mercaptophenyl)acetamide (Table 1, **3b**, see later): Yellow solid; 93% yield; IR (KBr) ν 3275, 2925, 2857, 1664, 1575, 1515, 1431, 1290, 752 cm^{-1} ^{1}H NMR (500 MHz, $CDCl_3$): δ_H (ppm) = 1.68 (s, 1H), 2.25 (s, 3H), 7.07 (t, 1H), 7.31 (dd, J = 16.9–7.2 Hz, 1H), 7.70 (dd, J = 20.1–6.3 Hz, 1H), 8.27 (s, 1H), 8.28 (d, J = 7.4 Hz, 1H).

N-(4-hydroxyphenyl)acetamide (Table 1, **3c**, see later): Dark brown solid; 92% yield; IR (KBr): ν 3322, 3161, 1654, 1614, 1562, 1507, 1437, 1369, 1231, 1108, 802, 682 cm^{-1}. ^{1}H NMR (250 MHz, DMSO): δ_H (ppm) = 1.82 (s, 3H), 6.57 (d, J = 7.7 Hz, 2H), 7.24 (d, J = 8.0 Hz, 2H), 8.99 (s, 1H), 9.53 (s, 1H).

3-acetamidobenzoic acid (Table 1, **3d**, see later): White solid; 95% yield; IR (KBr) ν 3339, 2927, 1706, 1639, 1559, 1486, 1256, 725 cm^{-1}. ^{1}H NMR (250 MHz, DMSO): δ_H (ppm) = 2.10 (s, 3H), 7.34 (t, J = 7.7 Hz, 1H), 7.64 (d, J = 7.5 Hz, 1H), 7.87 (d, J = 7.7 Hz, 1H), 7.98 (s, 1H), 8.17 (s, 1H), 9.97 (s, 1H).

N-benzylacetamide (Table 1, **3e**, see later): White solid; 92% yield; mp 58–60 °C; IR (KBr): ν 3291, 3084, 2926, 2855, 1641, 1550, 1442, 1366, 1287, 1080, 1025,

Table 1 Fe_3O_4@Chitosan-TCT-Salen–Cu(II) catalyzed acylation of amines

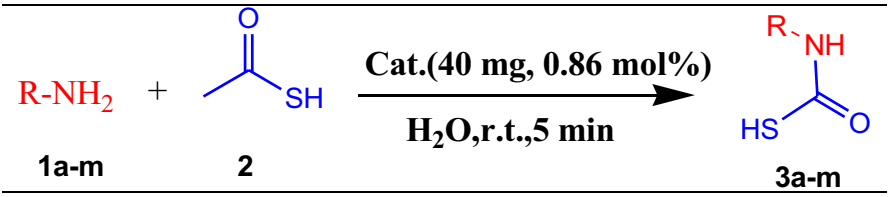

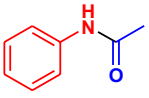

3a, 97%

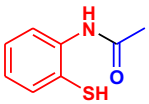

3b,99%

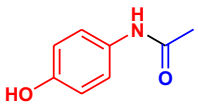

3c,92%

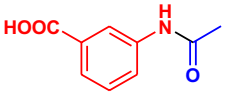

3d,97%

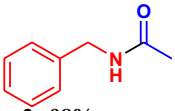

3e,98%

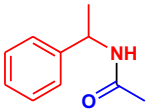

3f,92%

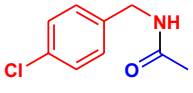

3g,98%

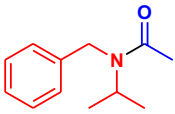

3h,90%

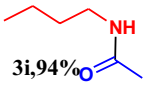

3i,94%

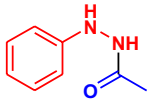

3j,91%

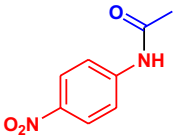

3k,81%

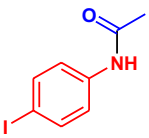

3l,93%

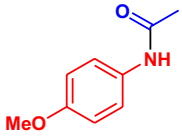

3m,95%

[a]Reaction conditions: amine (1 mmol), thioacetic acid (1 mmol), catalyst (40 mg), water (1 mL), room temperature, 5 min

[b]Isolated yield

742, 693 cm^{-1}. ^1H NMR (400 MHz, $CDCl_3$): δ_H (ppm) = 7.30–7.37 (m, 5H), 5.83 (br s, 1H), 4.45 (s, 2H), 2.05 (s, 3H).

N-(1-phenylethyl)acetamide (Table 1, **3f**, see later): White solid; 90% yield; IR (KBr): ν (cm^{-1}) 3279, 3044, 2978, 2865, 1668, 1530, 1382, 1262, 1088; cm^{-1}. ^1H NMR (500 MHz, Chloroform-d): δ_H (ppm) = 7.43–7.28 (m, 5H), 5.93 (s, 1H), 5.14 (p, J = 7.0 Hz, 1H), 1.99 (s, 3H), 1.50 (d, J = 6.9 Hz, 3H).

N-(4-chlorobenzyl)acetamide (Table 1, **3g**, see later): White solid; 95% yield; IR (KBr): ν 3277, 3079, 2927, 1640, 1551, 1488, 1455, 1374, 1286, 1090, 1015, 811, 598 cm^{-1}. ^1H NMR (500 MHz, Chloroform-d): δ_H (ppm) = 7.28 (d, J = 7.9 Hz, 2H), 7.18 (s, 2H), 6.28 (s, 1H), 4.35 (d, J = 5.9 Hz, 2H), 2.00 (s, 3H).

N-isopropyl-N-phenylacetamide (Table 1, **3h**, see later): Yellow oil, 91% yield; IR (KBr) ν 3437, 2926, 2856, 1642, 1420, 1263, 1202, 722 cm^{-1}. ^1H NMR (500 MHz, Chloroform-d): δ_H (ppm) = 7.31–7.22 (m, 6H), 4.49 (s, 2H), 4.15 (hept, J = 6.7 Hz, 1H), 2.04 (s, 3H), 1.12 (d, J = 6.8 Hz, 6H).

N-butylacetamide (Table 1, **3i**, see later): Yellow oil, 92% yield; IR (KBr): ν 3295, 2933, 2869, 1649, 1555, 1445, 1372, 1295, 735 cm^{-1}. ^1H NMR (500 MHz, Chloroform-d): δ_H (ppm) = 5.97 (s, 1H), 3.21 (td, J = 7.2, 5.7 Hz, 2H), 1.95 (s, 3H), 1.46 (p, J = 7.3 Hz, 2H), 1.33 (h, J = 7.3 Hz, 2H), 0.90 (t, J = 7.4 Hz, 3H).

N'-phenylacetohydrazide (Table 1, **3j**, see later): Pale brown solid;89% yield; mp 129–132 °C; IR (KBr): ν 3287, 3234, 3031, 2928, 1665, 1643, 1597 cm^{-1}. ^1H NMR (500 MHz, DMSO): δ_H (ppm) = 2.02 (s, 3H), 7.00 (t, J = 7.4, 7.3 Hz, 1H), 7.26 (t, J = 7.5, 8.3 Hz, 2H), 7.56 (d, J = 7.6 Hz, 2H), 9.94 (s, 1 H).

N-(4-nitrophenyl)acetamide (Table 1, **3k**, see later): Yellow solid; 80% yield; mp 101–103 °C; IR (KBr) ν 3358, 2960, 2925, 1628, 1596, 1477, 1304, 1261, 804 cm^{-1}. ^1H NMR (500 MHz, Chloroform-d): δ_H (ppm) = 8.24 (d, J = 8.7 Hz, 2H), 7.72 (d, J = 8.7 Hz, 2H), 7.53 (s, 1H), 2.27 (s, 3H).

N-(4-iodophenyl)acetamide (Table 1, **3l**, see later): White solid; 92% yield; mp 182–187 °C; IR (KBr) ν 3293, 2923, 2855, 1662, 1602, 1546, 1437, 1375, 1317, 1260, 752 cm^{-1}. ^1H NMR (500 MHz, Chloroform-d): δ_H (ppm) = 7.64 (d, J = 10.0 Hz, 2H), 7.30 (d, J = 10.0 Hz, 2H), 7.16 (s, 1H), 2.20 (s, 3H).

N-(4-methoxyphenyl)acetamide (Table 1, **3m**, see later): White solid; 94% yield; IR (KBr) ν 3445, 2925, 2855, 1647, 1512, 1455, 1250, 1023, 817 cm^{-1}. ^1H NMR (500 MHz, DMSO): δ_H (ppm) = 1.99 (s, 3H), 3.69 (s, 3H), 6.84 (d, J = 9.0 Hz, 2H), 7.46 (d, J = 8.9 Hz, 2H), 9.74 (s, 1H).

Results and discussion

Schematic pathway for preparation of Fe_3O_4@Chit-TCT-Salen–Cu(II) is illustrated in Scheme 1. Every intermediate in the synthetic pathway was characterized using FT-IR spectroscopy (Fig. 1). Characteristic peaks of chitosan are observed in Fig. 1a. Absorption at 3436 cm^{-1} is ascribed to the OH stretching frequency, which overlaps the NH_2 stretching ones [54–58]. The carbonyl stretching vibration of amide groups and C=N stretching of bonded cyanuric chloride appears in about the 1600–1700 cm^{-1} region [59]. The FT-IR spectrum of ethylenediamine-grafted Cht-TCT depicted in Fig. 1b shows an enlargement of peaks at 1590 cm^{-1} and 3400 cm^{-1}

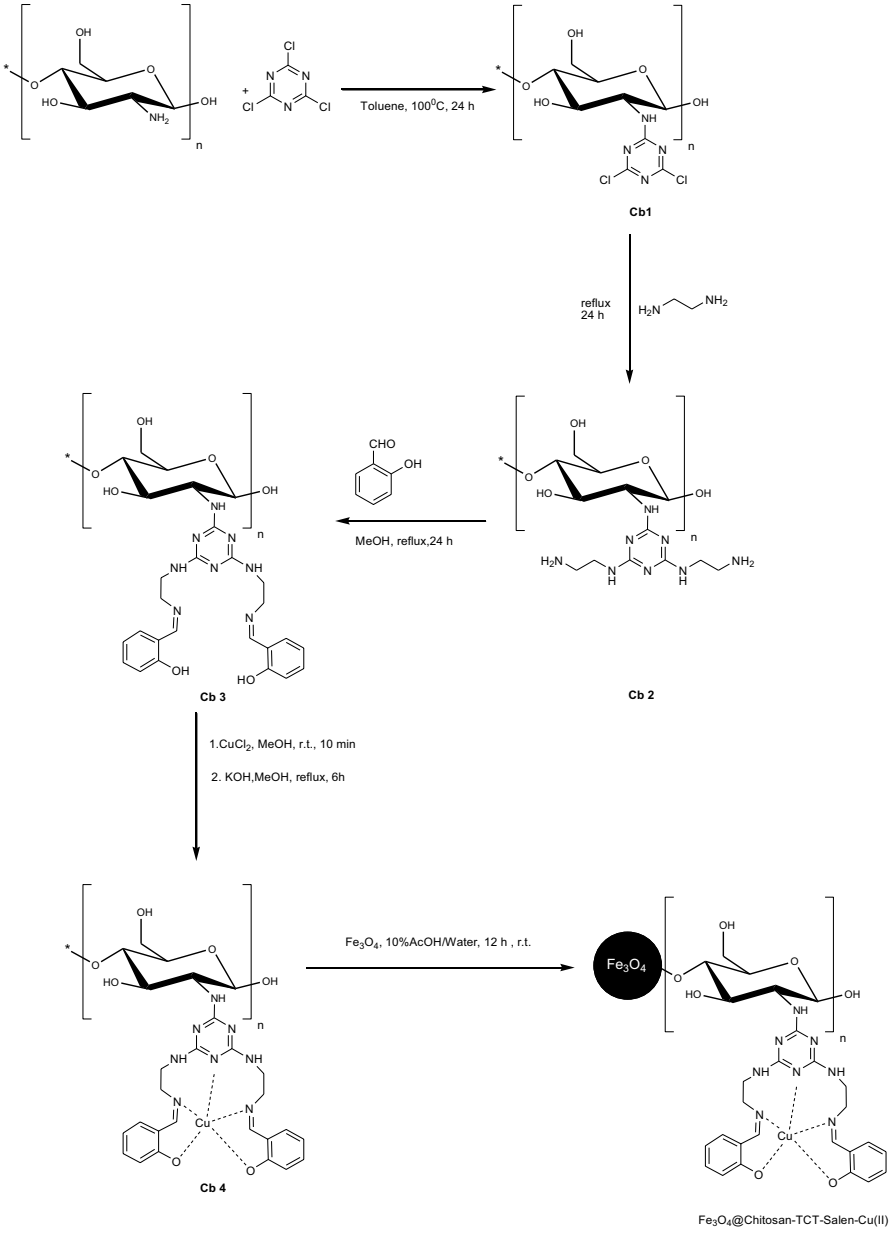

Scheme 1 Pathway to the synthesis of Fe_3O_4@Chitosan-TCT-Salen–Cu(II) nanoparticles

due to addition of pendant groups bearing NH_2 functionality [54–58]. The Schiff base absorption bands are shown in Fig. 1c. Peaks at 1634 cm^{-1} and 1412 cm^{-1} can be attributed to C=N stretching of the azomethine group and C=C stretching of the aromatic ring, respectively [59]. Coordination of the prepared ligand to Cu(II) ions

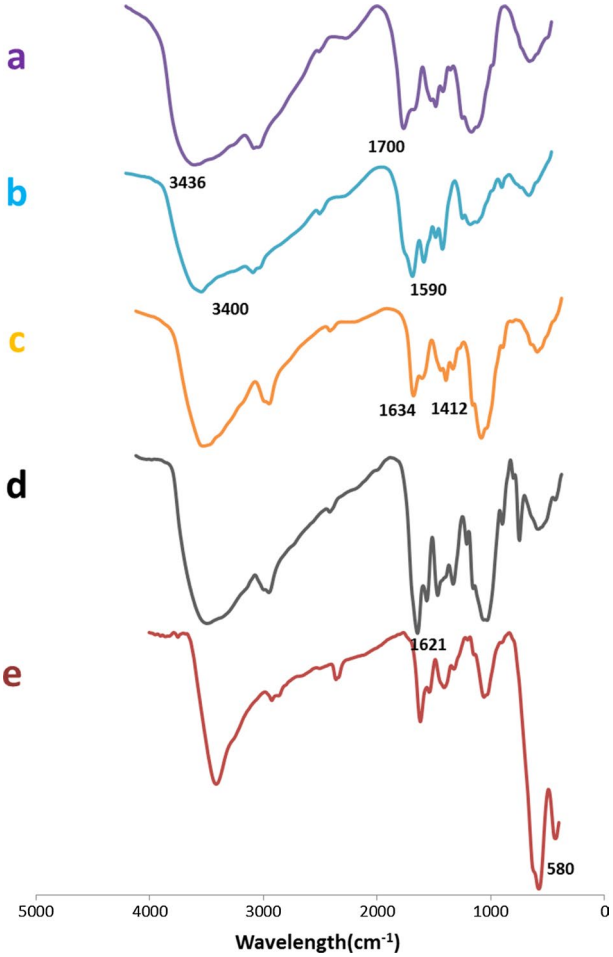

Fig. 1 FT-IR spectra of (a) Cb1, (b) Cb 2, (c) Cb3, (d) Cb4, (e) Fe_3O_4@Chitosan-TCT-Salen–Cu(II)

shifts the peak related to C=N to a lower frequency, i.e., 1621 cm^{-1} as compared to the free ligand (Fig. 1d) [60]. The FT-IR spectra of the final target nanoparticles are depicted in Fig. 1e, showing good accordance with the free complex absorption peaks, although intrinsic bands of magnetite at 580 cm^{-1} and overlapped 3400 cm^{-1} are also observed [61].

The crystalline structure of the magnetite core of the nanoparticles was verified by X-ray diffraction (XRD) patterns as shown in Fig. 2. The diffraction peaks of 21.38, 35.27, 41.62, 50.71, 63.28, 67.64 and 74.6 are related to the crystal faces (111), (220), (311), (400), (422), (511) and (440), respectively. These peaks are in acceptable agreement with those of JCPDS card no. 75-0033 which confirms no alteration of the spinel structure after modification of the magnetite nanoparticles with the metal complex. Furthermore, the XRD patterns of chitosan and every

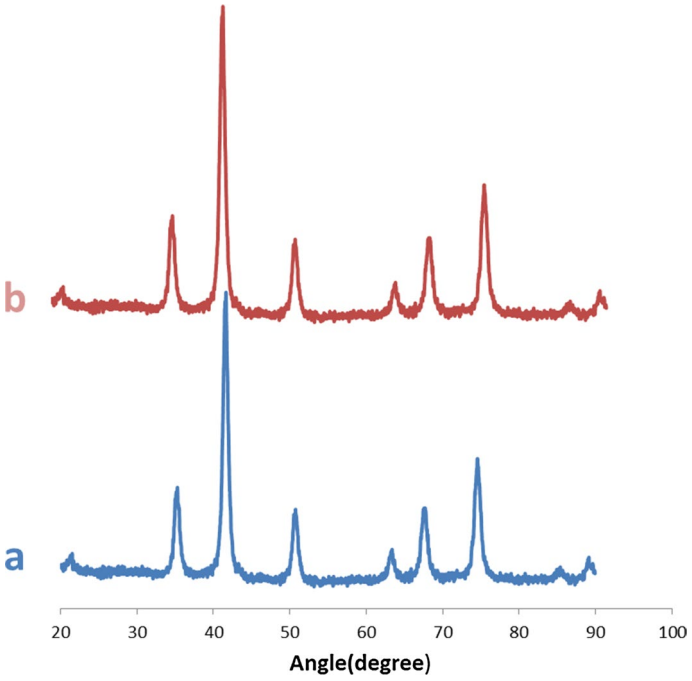

Fig. 2 XRD patterns of (a) Fe_3O_4 and (b) Fe_3O_4@Chitosan-TCT-Salen–Cu(II)

intermediate in the synthetic pathway are illustrated in Fig. 3. Chitosan exhibited low crystallinity as indicated by a broad band at about 20. The intermediates, Cb1, Cb2, Cb3 and Cb4, which are chemically modified chitosan, show sn even greater decrease in crystallinity [62].

Thermogravimetric analysis was conducted to determine the organic moieties content of the nanoparticles (Fig. 4). For this purpose, the nanoparticles were heated at a rate of 10 °C/min within the range of 25–800 °C under a flow of compressed N_2 gas. The first weight loss below 200 °C is due to evaporation of chemisorbed materials, presumably moisture. As the sample temperature is increased to over 400 °C, disintegration of the organic ligands of the immobilized complex on the surface of nanoparticels occurs which contributes to about 15% (W/W) of the total sample size [63].

The magnetic properties of the prepared nanoparticles were measured by vibrating sample magnetometry (Fig. 5). The magnetization curve of the nanoparticles ($emug^{-1}$) as a function of the applied magnetic field between − 10,000 and + 10,000 Oe shows a magnetic saturation of about 30 emu g^{-1}. The superparamangetic nature of the nanoparticles is demonstrated by the zero remanence and coercivity of the magnetization curve, which facilitate its easy separation from the reaction mixture with an external magnet [64].

The transmission electron microscopy micrograph of the prepared nanoparticles shows almost spherical particles (Fig. 6). The size of the particles is in the range of 5–16 nm. The average particle size was calculated using Scherrer's formula [66]:

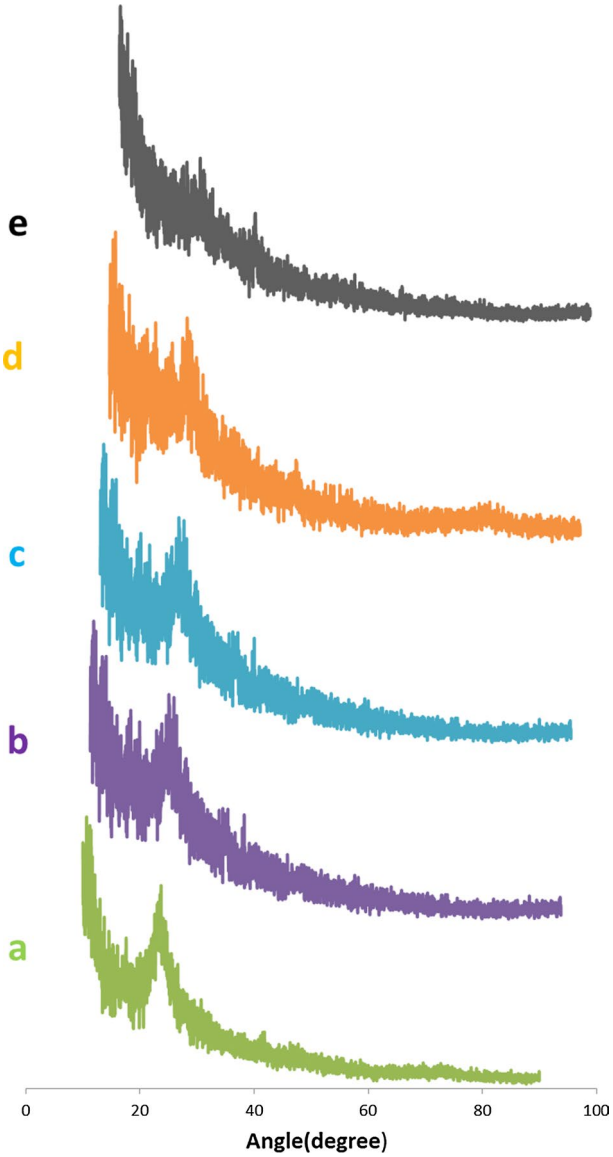

Fig. 3 XRD patterns of (a) Chitosan, (b) Cb1, (c) Cb2, (d) Cb3, (e) Cb4

$\tau = K\lambda/\beta\cos\theta$, where τ is the mean size of crystalline phase, K is a dimensionless shape factor, which is close to unity. λ is the X-ray wavelength, β is the FWHM of diffraction peak and θ is the diffraction angle. The resulting mean particle size from this equation is 16.5 nm.

A scanning electron microscopy image of the synthesized nanoparticles is shown in Fig. 7, and indicates uniform nanoparticles.

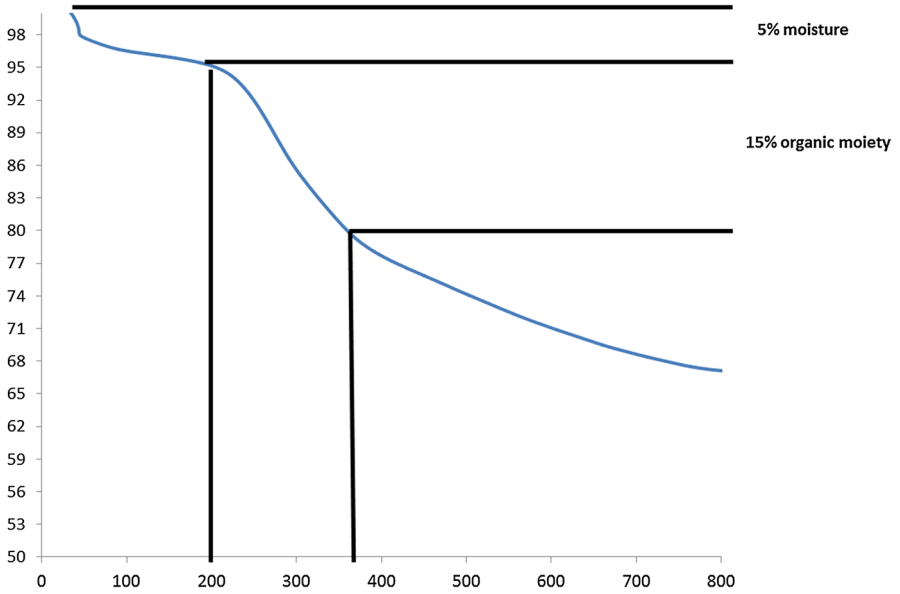

Fig. 4 Thermogravimetric analysis of Fe_3O_4@Chitosan-TCT-Salen–Cu(II)

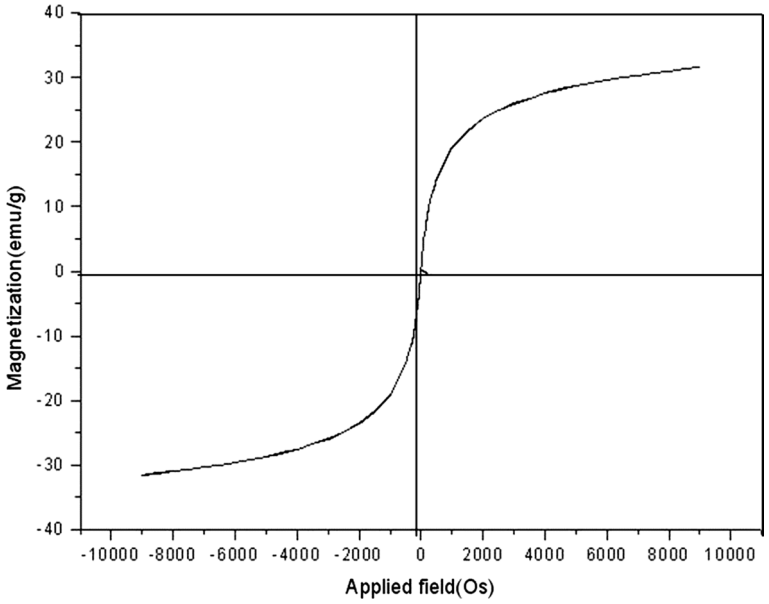

Fig. 5 Vibrating sample magnetometry of Fe_3O_4@Chitosan-TCT-Salen–Cu(II)

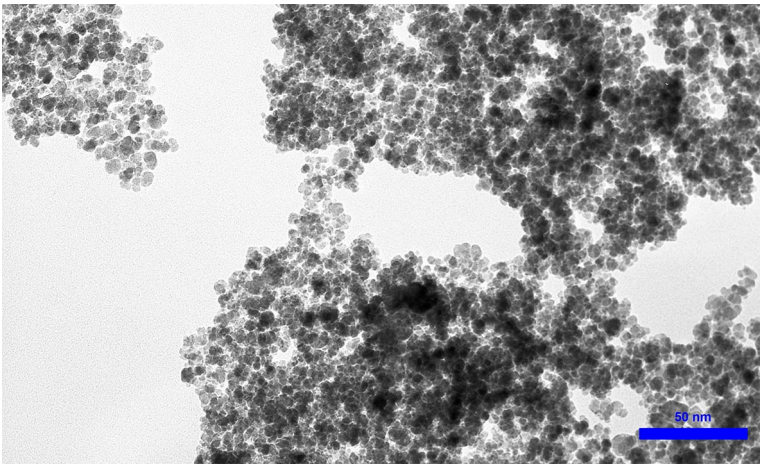

Fig. 6 Transmission electron microscopy micrograph of Fe_3O_4@Chitosan-TCT-Salen–Cu(II)

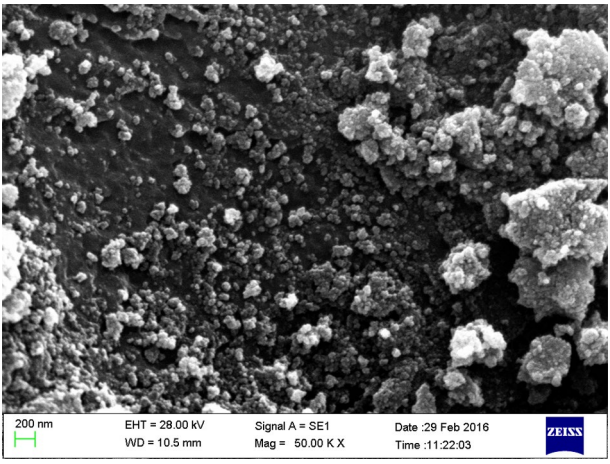

Fig. 7 Scanning electron microscopy image of Fe_3O_4@Chitosan-TCT-Salen–Cu(II)

The presence of the expected elements in the prepared nanoparticles was deduced using EDS which is outlined in Fig. 8. The presence of Fe, C, N, O and Cu elements on the surface of the nanoparticles confirms the successful synthesis and immobilization of the copper complex. Furthermore, the precise amount of the copper content of the nanoparticles was determined using ICP analysis as 0.216 mmol per g.

The catalytic activity of the prepared nanoparticles was tested in the *N*-acetylation of amines with thioacetic acid. To achieve the best reaction condition, *N*-acetylation of aniline was chosen as the probe reaction (Scheme 2). Then, the reaction was carried out under various conditions of solvent and catalyst loadings (Table 2). As most of the organic materials are soluble in dichloromethane, the first run was performed

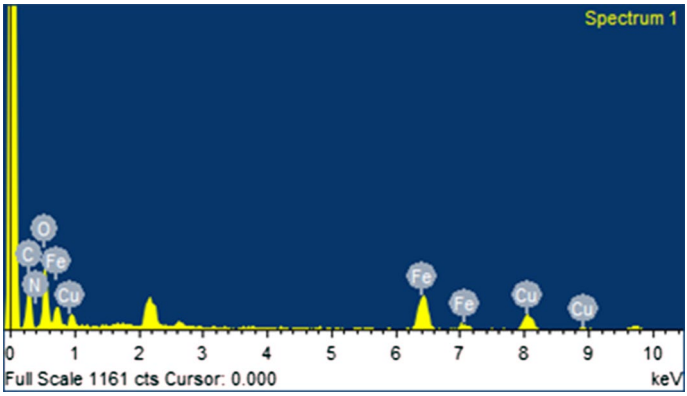

Fig. 8 EDS analysis of Fe_3O_4@Chitosan-TCT-Salen–Cu(II)

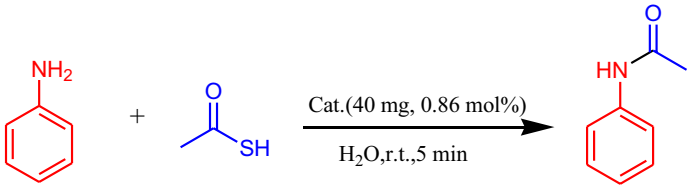

Scheme 2 Acetylation of aniline

Table 2 Optimization of reaction conditions of aniline acetylation

Entry	Catalyst (mg)	Solvent	Yield (%)[a]
1	40	CH_2Cl_2	48
2	40	CH_3CN	68
3	40	EtOH	85
4	40	MeOH	96
5	40	H_2O	97
6	–	H_2O	–
7	40[b]	H_2O	50
8	80	H_2O	99

Reaction conditions: aniline (1 mmol), thioacetic acid (1 mmol), solvent (1 mL)

[a]Isolated yield

[b]Fe_3O_4 nanoparticles

in this solvent; however, the practical yield was moderately low (entry 1). The result of the first test implied that a more polar solvent is needed to enhance the catalyst efficiency. Thus, the effects of common laboratory polar solvents like acetonitrile, ethanol, methanol and water were examined (entries 2–5). It is evident that the more polar the solvent, the more the yield of the desired product. Therefore, water was

selected as the reaction medium, due to the higher product yield and also because it is a sustainable solvent. The requirement of catalyst presence for the reaction to proceed was verified, as no product was detected in the absence of the catalyst (entry 6). In order to ensure that the copper(II) ion has a necessary role in the catalytic process, the reaction was conducted with bare magnetite nanoparticles, which resulted in a much lower yield (entry 7). Furthermore, it was observed that increasing the amount of catalyst had a negligible effect on the obtained yield (entry 8).

As mentioned earlier, chemoselective protection of amino groups is a rather difficult process when other nucleophilic functionalities are present. To prove chemoselectivity of the copper-catalyzed acetylation method, S, OH and carboxylic substituted anilines were examined (**3b–d**). The desired N-acetylated products were formed and no O or S acetylation or sulfide dimerization was observed. The protocol is also applicable to benzyl amines and to secondary and aliphatic ones (**3e–i**). Furthermore, regioselectivity of the method under investigation was checked. Phenyl hydrazine was reacted under similar reaction conditions and only the primary amino group was protected (**3j**).

To understand the tolerance of the protocol to electronic effects of the substituents, both electron-withdrawing (nitro and halogen) and electron-donating (methoxy) groups were undertaken as the reaction substrates (3 k m). It can be concluded that groups with a resonance electron-withdrawing character e.g. $–NO_2$ will decrease the product yield due to diminishing the nucleoophilic power of the amino group.

The model reaction (Scheme 2) was carried out under the optimized conditions. After the reaction was completed, the catalyst was removed from the medium using an external magnet, washed twice with water and dichloromethane, and dried at ambient temperature for reuse in the next run. This process was repeated 6 times until unsatisfactory results were obtained (Fig. 9). A hot filtration test was used to check the heterogeneity of the catalyst. After 2 min from the beginning of the reaction, the catalyst was removed and the reaction mixture was left being stirred for another 2 h, but no more product was formed during this period. Moreover, leaching of copper ions was studied using ICP analysis of the reaction mixture. The result showed no detection of the Cu element. Additionally, the obtained acylation

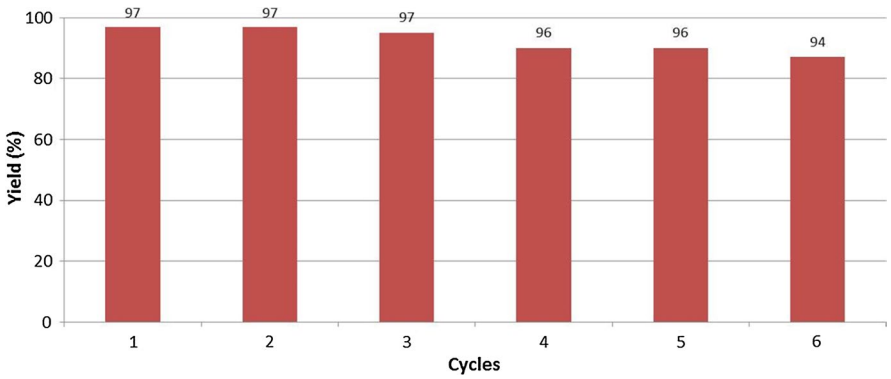

Fig. 9 Recycling of Fe_3O_4@Chitosan-TCT-Salen–Cu(II) in the *N*-acetylation of aniline

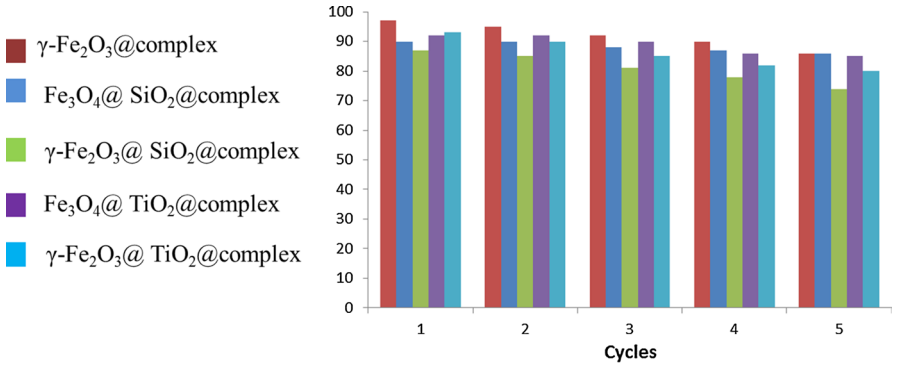

Fig. 10 Recycling of different complex magnetic supports in the *N*-acetylation of aniline

products were dissolved in ethyl acetate, and, after extraction with water, no residual Cu content was detected in the aqeuoeus layer using ICP analysis.

Furthermore, the effect of variations in the magnetic core and shell of the nanoparticles as the complex support was studied (Fig. 10). γ-F_2O_3 showed the greatest yields as compared to the others, which may be attributed to its low molecular weight; hence, more Cu content is present in the reaction when the same catalyst amount is used. However, catalysts with maghemite as the core showed further decrease in their activity which is due to more loss of the catalyst in every step of magnetic decanting. Hence, the choice of bare magnetic nanoparticles was reasonable due to their efficient recyclability and straightforward synthetic procedure.

The efficiency of the prepared nanocatalyst was compared to the reported catalyst in our groups or others for the acetylation of aniline using thioacetic acid and acetic acid as the acetylating agent (Table 3). It is clear that the amount of copper loading needed for catalysis is considerably diminished in the reported protocol. Also, thioacetic acid is a considerably more efficient agent for amine acetylation.

Scheme 3 presents a proposed mechanism of the *N*-acetylation reaction. First, the C–S bond of thioacetic acid is weakened through chelation to copper ions. Moreover, the carbonyl group electrophilic character is enhanced as it is complexed to

Table 3 Fe_3O_4@Chitosan-TCT-Salen–Cu(II)-catalyzed acylation of amines

Entry	Catalyst (mg)	Solvent	Yield (%)
1	$CuSO_4$ (30%) [41]	MeOH	92
2	MNP-GAA-Cu(II) (2.2%) [62]	H_2O	95
3	Fe_3O_4@SiO_2/Salen–Cu(II) (40 mg)	H_2O	96
4	Fe_3O_4@SiO_2@Mo–Schiff base (40 mg)	H_2O	97
5	Chitosan-TCT-Salen–Cu(II) (40 mg)	H_2O	99
6	MNP-Chit-Salen–Cu(II) (0.86%)	H_2O	97
7	MNP-Chit-Salen–Cu(II) (0.8%)[a]	H_2O	20

[a]Acetic acid as acetylating agent

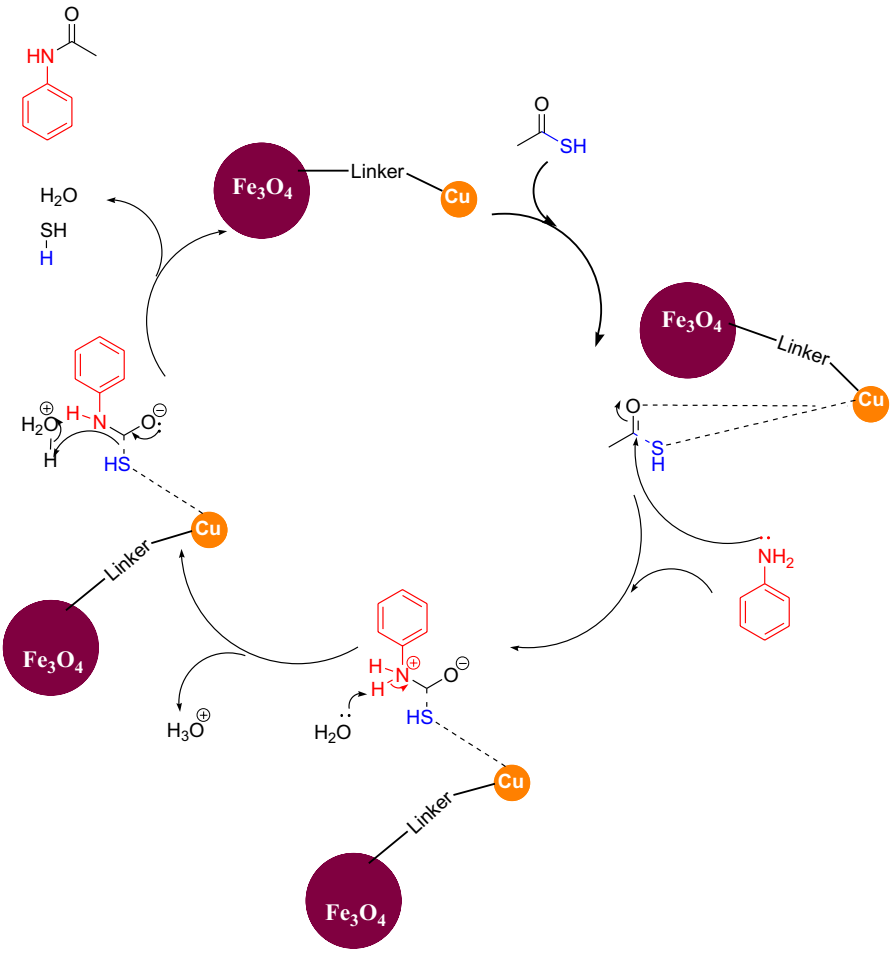

Scheme 3 Proposed mechanism for amine acylation

Cu(II). In the next step, the amino group attaches to the carbonyl group. Finally, the N-acetylated product is released with the simultaneous evolution of hydrogen sulfide gas.

Conclusions

In summary, a copper(II)–salen complex was supported on the surface of magnetite nanoparticles. These nanoparticles were applied in the *N*-acetylation of anilines using thioacetic acid as the acetylating agent. The protocol is highly chemo- and region-selective. Furthermore, it is an environmentally benign method, as it is performed in water. The catalyst is magnetically recoverable for 6 consecutive cycles

with no significant decrease in catalytic activity. Moreover, the purification process contains simple work-up with no need for chromatographic separations.

Acknowledgement We acknowledge Tarbiat Modares University for partial support of this work.

References

1. P.R. Sultane, T.B. Mete, R.G. Bhat, Org. Biomol. Chem. **12**, 261 (2014)
2. P.M. Dewick, *Medicinal Natural Products: A Biosynthetic Approach* (Wiley, West Sussex, 2009), p. 311
3. M. Nasrollahzadeh, New J. Chem. **38**, 5544 (2014)
4. D. Chusov, B. List, Angew. Chem. Int. Ed. **53**, 5199 (2014)
5. D. Seildel, Acc. Chem. Res. **48**, 317 (2015)
6. A. Peeters, R. Ameloot, D.E. De Vos, Green Chem. **15**, 1550 (2013)
7. J. Li, M.J. Lear, Y. Kawamoto, S. Umemiya, A.R. Wong, E. Kwon, I. Sato, Y. Hayashi, Angew. Chem. Int. Ed. **54**, 12986 (2015)
8. J.T. Reeves, M.D. Visco, M.A. Marsini, N. Grinberg, C.A. Busacca, A.E. Mattson, C.H. Senanayake, Org. Lett. **17**, 2442 (2015)
9. R. Villano, M.R. Acocella, G. Guerra, ChemistrySelect **2**, 10559 (2017)
10. A. Leoncini, J. Huskens, W. Verboom, Synlett **27**, 2463 (2016)
11. S.L. Montgomery, J.M. Sanchez, M.P. Thompson, G.A. Aleku, B. Dominguez, N.J. Turner, Angew. Chem. Int. Ed. **56**, 10491 (2017)
12. R.M. McFadden, B.M. Stoltz, J. Am. Chem. Soc. **128**, 7738 (2006)
13. I.S. Young, P.S. Baran, Nat. Chem **1**, 193 (2009)
14. W.R. Gutekunst, P.S. Baran, Chem. Soc. Rev. **40**, 1976 (2011)
15. V. Hickmann, M. Alcarazo, A. Furstner, J. Am. Chem. Soc. **132**, 11042 (2010)
16. P.G.M. Wuts, T.W. Greene, *Green's Protective Groups in Organic Synthesis* (Wiley, Hookben, 2007), p. 773
17. R.C. Larock, *Comprehensive Organic Transformations* (Wiley, Weinheim, 1989), p. 150
18. K. Phukan, M. Ganguly, N. Devi, Synth. Commun. **39**, 2694 (2009)
19. C.L. Allen, J.M. Williams, Chem. Soc. Rev. **40**, 3405 (2011)
20. N.O. Sonntag, Chem. Rev. **52**, 237 (1953)
21. R. Murugan, E.F. Scriven, ChemInform. **35**, e3744 (2004)
22. R.P. Wurz, Chem. Rev. **107**, 5570 (2007)
23. M. Sato, K. Matsushima, H. Kawanami, M. Chatterjee, T. Yokoyama, Y. Ikuhsima, T.M. Suzuki, Lab Chip **9**, 2877 (2009)
24. A. Vogel, *Practical Organic Chemistry* (Langman Scientific & Technical and Wiley, New York, 1989), p. 708
25. J. March, *Advanced Organic Chemistry* (Wiley, New York, 1992), p. 416
26. G. Hofle, W. Steglich, H. Vorbruggen, Angew. Chem. Int. Ed. Engl. **17**, 569 (1978)
27. E. Vedejs, N.S. Bennett, L.M. Conn, S.T. Diver, K. Gingras, S. Lin, P.A. Oliver, M.J. Peterson, J. Org. Chem. **58**, 7286 (1993)
28. R. Murugan, E.F.V. Scriven, Aldrichimica Acta **36**, 23 (2003)
29. A.R. Katritzky, H.Y. He, K. Suzuki, J. Org. Chem. **65**, 8210 (2000)
30. J.R. Phillips, *Thiolacetic Acid. e-EROS Encyclopedia of Reagents for Organic Synthesis* (Wiley-VCH, Weinheim, 2001)
31. P. Wang, S.J. Danishefsky, J. Am. Chem. Soc. **132**, 17045 (2010)
32. P. Wang, X. Li, J. Zhu, J. Chen, Y. Yuan, X. Wu, S.J. Danishefsky, J. Am. Chem. Soc. **133**, 1597 (2011)
33. W. Wu, Z. Zhang, L.S. Liebeskind, J. Am. Chem. Soc. **133**, 14256 (2011)
34. N. Shangguan, S. Katukojvala, R. Greenberg, L.J. Williams, J. Am. Chem. Soc. **125**, 7754 (2003)
35. Y. Rao, X. Li, S.J. Danishefsky, J. Am. Chem. Soc. **131**, 12924 (2009)
36. D. Crich, I. Sharma, Angew. Chem. Int. Ed. **48**, 2355 (2009)
37. D. Crich, K. Sana, S. Guo, Org. Lett. **9**, 4423 (2007)
38. J. Pan, N.O. Devarie-Baez, M. Xian, Org. Lett. **13**, 1092 (2011)

39. D. Crich, K. Sasaki, Org. Lett. **11**, 3514 (2009)
40. R. Liu, L.E. Orgel, Nature **389**, 52 (1997)
41. S.M. Mali, R.D. Bhaisare, H.N. Gopi, J. Org. Chem. **78**, 5550 (2013)
42. H. Liu, Z. Liyun, Y. Yunfei, X. Zhifang, C. Kai, Q. Shengxiang, T. Haibo, ACS Catal. **6**, 3 (2016)
43. W. Chen, S. Jiaan, H. Miao, Y. Wanwan, A.G. Marc, A.H. Richard, Y. Yongping, Chem. Sci. **4**, 3 (2013)
44. M. Munoz, Z.M. de Pedro, J.A. Casas, J.J. Rodriguez, Appl. Catal. B **176–177**, 249 (2015)
45. S. Urus, S. Purtas, G. Ceyhan, F. Tumer, Chem. Eng. J. **220**, 420 (2013)
46. B.S. Lane, K. Burgess, Chem. Rev. **103**, 2457 (2003)
47. R. Skoda-Foldes, L. Kollar, A. Arcadi, J. Mol. Catal. **101**, 37 (1995)
48. L.P.C. Nielson, C.P. Stevenson, D.G. Backmond, E.N. Jacobsen, J. Am. Chem. Soc. **126**, 1360 (2004)
49. G. Righi, C. Bonini, Synthesis **3**, 225 (1994)
50. J. Lopez, S. Liang, X.R. Bu, Tetrahedron Lett. **39**, 4199 (1998)
51. Y. He, C. Cai, Catal. Commun. **12**, 678 (2011)
52. M.E.I. Badawy, E.I. Rabea, Int. J. Carbohydr. Chem. **2011**, 29 (2011)
53. M. Rinaudo, Prog. Polym. Sci. **31**, 603 (2006)
54. E. Yazdani, K. Azizi, A. Nakisa, A. Heydari, Org. Chem. Res. **1**, 27 (2015)
55. K. Azizi, J. Azarnia, M. Karimi, E. Yazdani, A. Heydari, Synlett **27**, 1810 (2016)
56. A. Nakisa, M. Karimi, E. Yazdani, A. Heydari, Appl. Organometal. Chem. **31**, e3674 (2017)
57. M.K. Miraki, M. Arefi, E. Yazdani, S. Abbasi, M. Karimi, K. Azizi, A. Heydari, ChemistrySelect **1**, 6328 (2016)
58. L. Ghandi, M.K. Miraki, I. Radfar, E. Yazdani, A. Heydari, ChemistrySelect **3**, 1787 (2018)
59. E.C.N. Lopez, K.S. Sousa, C. Airoldi, Thermochim. Acta **483**, 21 (2009)
60. K. Abdollahi, F. Yazdani, R. Panahi, Int. J. Biol. Macromol. **94**, 396 (2017)
61. M. Esmaeilpour, J. Javidi, F.N. Dodeji, M.M. Abarghou, Transit. Met. Chem. **39**, 797 (2014)
62. M.K. Miraki, E. Yazdani, L. Ghandi, K. Azizi, A. Heydari, Appl. Organometal. Chem. **31**, e3744 (2017)
63. K. Azizi, N. Esfandiary, M. Karimi, E. Yazdani, A. Heydari, RSC Adv. **6**, 89313 (2016)
64. E. Ghonchepour, E. Yazdani, D. Saberi, M. Arefi, A. Heydari, Appl. Organometal. Chem. **31**, e3822 (2017)
65. L. Liu, Y. Ai, D. Li, L. Qi, J. Zhou, Z. Tang, Z. Shao, Q. Liang, H.B. Sun, ChemCatChem. **9**, 3131 (2017)
66. A. Patterson, Phys. Rev. **56**, 978 (1939)